Structural analysis of emerin, an inner nuclear membrane protein mutated in X-linked Emery–Dreifuss muscular dystrophy

Nicolas Wolff[a,1], Bernard Gilquin[a], Karine Courchay[a], Isabelle Callebaut[b], Howard J. Worman[c], Sophie Zinn-Justin[a,*]

[a] *Département d'Ingénierie et d'Etudes des Protéines, CEA Saclay, 91191 Gif-sur-Yvette, France*
[b] *Laboratoire de Minéralogie-Cristallographie Paris, CNRS UMR 7590, Universités Paris 6/Paris 7, Case 115, 4 place Jussieu, 75252 Paris Cedex 05, France*
[c] *Departments of Medicine and of Anatomy and Cell Biology, College of Physicians and Surgeons, Columbia University, New York, NY 10032, USA*

Received 10 May 2001; accepted 15 June 2001

First published online 4 July 2001

Edited by Hans Eklund

Abstract Like Duchenne and Becker muscular dystrophies, Emery–Dreifuss muscular dystrophy (EDMD) is characterized by myopathic and cardiomyopathic abnormalities. EDMD has the particularity of being linked to mutations in nuclear proteins. The X-linked form of EDMD is caused by mutations in the emerin gene, whereas autosomal dominant EDMD is caused by mutations in the lamin A/C gene. Emerin colocalizes with lamin A/C in interphase cells, and binds in vitro to lamin A/C. Recent work suggests that lamin A/C might serve as a receptor for emerin. We have undertaken a structural analysis of emerin, and in particular of its N-terminal domain, which is comprised in the emerin segment critical for binding to lamin A/C. We show that region 2–54 of emerin adopts the LEM fold. This fold was originally described in the two N-terminal domains of another inner nuclear membrane protein called lamina-associated protein 2 (LAP2). The existence of a conserved solvent-exposed surface on the LEM domains of LAP2 and emerin is discussed, as well as the nature of a possible common target.

Key words: Muscular dystrophy; Emerin; LEM domain; Nuclear magnetic resonance; Three-dimensional structure; Lamin

1. Introduction

Duchenne, Becker and Emery–Dreifuss muscular dystrophies all are distinguishable by myopathic and cardiomyopathic abnormalities (reviewed in [1,2]). The first two types arise due to genetic defects in the cytoskeletal/plasma membrane-associated protein dystrophin, which is part of the glycoprotein complex linking actin to the extracellular matrix. Emery–Dreifuss muscular dystrophy is linked to mutations in nuclear proteins, which suggests that its pathophysiology may be very different from the other types of muscular dystrophy [3,4]. It is due to genetic defects in an inner nuclear membrane protein named emerin [5] or in lamin A/C [6].

Human emerin is a serine-rich protein of 254 amino acids [5]. The sequence of emerin is composed of an N-terminal globular domain of about 50 residues, followed by a poly-Ser segment, then a region of 100 residues rich in hydrophobic amino acids comprising the nuclear localization signal [7,8], again a poly-Ser segment, and finally a C-terminal transmembrane region (Fig. 1). To date, more than 50 different pathogenic mutations have been described in emerin (http://www.path.cam.ac.uk/emd/mutation.html), most resulting in truncated proteins which are not expressed and others causing amino acid substitutions. Interestingly, despite the different mutations in Emery–Dreifuss muscular dystrophy, producing varying effects on emerin expression, the clinical phenotype of all the patients is similar.

The functions of inner nuclear membrane proteins are not completely known, although they are suggested to have a structural role in maintaining nuclear architecture [9]. Interactions of inner nuclear membrane proteins with nuclear lamina and chromatin have been reported in interphase cells. Lamin B receptor binds to B-type lamins and chromatin proteins [10,11], lamina-associated protein (LAP) 1 and 2 isoforms interact with specific types of lamina and chromatin [12–15], and emerin probably targets A-type and B-type lamins [16–19].

The intranuclear organization of the chromosomes is not altered in cells that lack emerin [20]. Thus, emerin is not necessary for localizing chromosomes at the nuclear periphery and the muscular dystrophy phenotype is not due to a grossly altered nuclear organization of the chromatin. Emerin has a role in cell cycle-dependent events, since it can occur in four differently phosphorylated forms, three of which appear to be associated with the cell cycle [21]. In interphase cells, emerin colocalizes with A-type lamin, whereas during mitosis, emerin becomes dispersed throughout the cell, no longer colocalizing with lamin. It then participates in the reconstitution of membranes around the daughter nuclei at telophase [22]. Phosphorylation of emerin may be involved in controlling these events.

Emerin was shown to be absent from the inner nuclear membrane in most patients with X-linked muscular dystrophy. Interestingly, emerin is also largely distributed in the

*Corresponding author. Fax: (33)-1-69 08 90 71.
E-mail address: szinn@cea.fr (S. Zinn-Justin).

[1] Present address: Laboratoire de Résonance Magnétique Nucléaire, CNRS URA 1129, Institut Pasteur, Paris, France.

Abbreviations: DQF-COSY, double quantum filtered correlated spectroscopy; HCA, hydrophobic cluster analysis; LAP, lamina-associated protein; NOESY, nuclear Overhauser effect spectroscopy; NMR, nuclear magnetic resonance; RMSD, root mean square deviation; TOCSY, total correlated spectroscopy

0014-5793/01/$20.00
PII: S0014-5793(01)02649-7

endoplasmic reticulum of cells lacking lamin A [17], suggesting that lamin A serves as a receptor for emerin in the nucleus. An interaction between lamin A and residues 1–188 of emerin was observed using biomolecular interaction analysis and monoclonal antibodies [18]. By the yeast two-hybrid system, region 384–566 at the C-terminus of lamin A was identified as essential for the interaction with emerin [19]. However, no structural data exist at an atomic resolution on the emerin/lamin A complex.

We here report a structural analysis of the inner nuclear membrane protein emerin. The work focuses on the emerin globular N-terminal domain, which has been described as containing a LEM motif by Lin et al. [23]. This domain is comprised in the region critical for emerin/lamin A interaction [18], and is involved in the interaction of emerin with the DNA binding protein BAF [15].

2. Materials and methods

2.1. Sample preparation

The LEM domain of emerin was predicted to include residues 1–44 [23]. It was extended in order to obtain a well-structured protein soluble at a millimolar concentration. The final sequence chosen for the structural study corresponds to residues 2–54 of emerin. The peptide numbering used in the following study goes from 1 to 53.

Chemical synthesis of the LEM domain was carried out in solid phase using the Fmoc strategy on an Applied Biosystems 431A. The protein was purified by HPLC on a semi-preparative Vydac C18 column from Merck, and its purity was checked on the corresponding analytic column in the same solvent conditions. Its molecular weight was measured by electrospray mass spectrometry. It was found to be consistent with the expected sequence.

For the analytic ultracentrifugation experiments, the protein concentration was 10–50 μM, and the solvent was a buffer of 1 mM sodium phosphate at pH 6.3. For the nuclear magnetic resonance (NMR) experiments, protein concentration was 1–1.5 mM. The solvent was a buffer of 20 mM sodium phosphate at pH 6.3. 3-(Trimethylsilyl)[2,2,3,3-$^2H_4$]propionate was added as a chemical shift reference. Two samples were prepared: the first sample was diluted in 90% H_2O, 10% D_2O and the second sample was diluted in 100% D_2O.

2.2. Analytic ultracentrifugation experiments

Sedimentation equilibrium was performed at 298 K on a Beckman Optima XLA ultracentrifuge using a AN 60 Ti rotor and cells with a 12 mm optical path length. Sample volumes of 100 μl were centrifuged at 30 000 and 40 000 rpm. Radial scans of absorbance at 274 nm were taken at 3 h intervals, and equilibrium was achieved after 60 h. Data were analyzed using the XL-A/XL-2 software supplied by Beckman.

2.3. NMR experiments

All experiments were carried out at 298 K on a Bruker 600 MHz or 800 MHz spectrometer. Two-dimensional double quantum filtered correlated spectroscopy (DQF-COSY) [24], total correlated spectroscopy (TOCSY) [25] and nuclear Overhauser effect spectroscopy (NOESY) [26] experiments were recorded. A DIPSI2 composite pulse was used for isotropic mixing during 80 ms in the TOCSY experiments. A set of NOESY experiments were carried out with mixing times of 60, 100, 140, and 180 ms, and using a preparation period of 2 s. The water signal was suppressed by a WATERGATE sequence [27]. All experiments were performed in hypercomplex mode. The spectra were recorded with 512 $t_1 \times 1024$ t_2 points (1024 $t_1 \times 4096$ t_2 for DQF-COSY). Data processing was carried out using XWIN-NMR (Bruker) and FELIX (Biosym Technologies, San Diego, CA, USA) programs.

One-dimensional spectra were recorded before and after each set of experiments, to ensure that the protein was not structurally modified with time.

2.4. Proton resonance frequency assignment

In order to assign each of the protein proton frequencies, spin systems were identified on the TOCSY spectra. Sequential assignment was essentially carried out on the basis of $HN_i-H\alpha_{i+1}$ and HN_i-HN_{i+1} nuclear Overhauser effect (nOe) interactions. All nonlabile protons were assigned except Hζ of Phe38. The backbone NH and side chain NH_2 were also assigned.

2.5. Experimental restraints

Proton–proton distance restraints were deduced from the analysis of the NOESY spectra recorded at different mixing times. The volumes of the nOe cross-peaks were integrated. For each peak, a build-up curve was constructed by fitting the experimental volumes to the following function of the mixing time: $f(\tau_m) = a\ \tau_m + b\ \tau_m^2$. The coefficient a was taken as a build-up rate of the corresponding nOe. Calibration of these dipolar correlation rates was achieved on the basis of the known range of dαN distances. The errors made on the distances were evaluated to 25%. When comparison of the distances deduced from peaks found on both sides of the diagonal and in both solvents (H_2O and D_2O) showed an error larger than 25%, an error equal to twice their root mean square deviation (RMSD) was used [28].

2.6. Structure calculation

A semi-automated iterative assignment procedure was applied for the assignment of the nOe and the construction of the three-dimen-

Table 1
Experimental restraints and structural statistics for the emerin N-terminal domain[a]

Number of experimental distance restraints	
Unambiguous	1209
Ambiguous	87
Number of violations higher than 0.5 Å	0
RMSD from ideal values	
Bond (Å)	0.0061 ± 0.0002
Angle (°)	0.980 ± 0.022
Energy (kcal/mol)	
Bond	33.2 ± 1.8
Angle	233.6 ± 10.3
vdW[b]	40.8 ± 4.9
nOe[c]	347.9 ± 14.1
Ramachandran analysis (for residues 1–43)[d]	
Residues in favored regions	63.8%
Residues in additional allowed regions	30.0%
Residues in generously allowed regions	5.9%
Residues in disallowed regions	0.3%
Coordinate precision (for residues 1–43, in Å) on backbone atoms	0.56 ± 0.11

[a]All values are averaged on the 10 X-PLOR structures.
[b]The van der Waals energy is calculated with a repel function and the paramallhdg parameters.
[c]The values of the square-well nOe are calculated with force constants of 50 kcal/mol/Å^2.
[d]Calculated with Procheck-nmr [34].

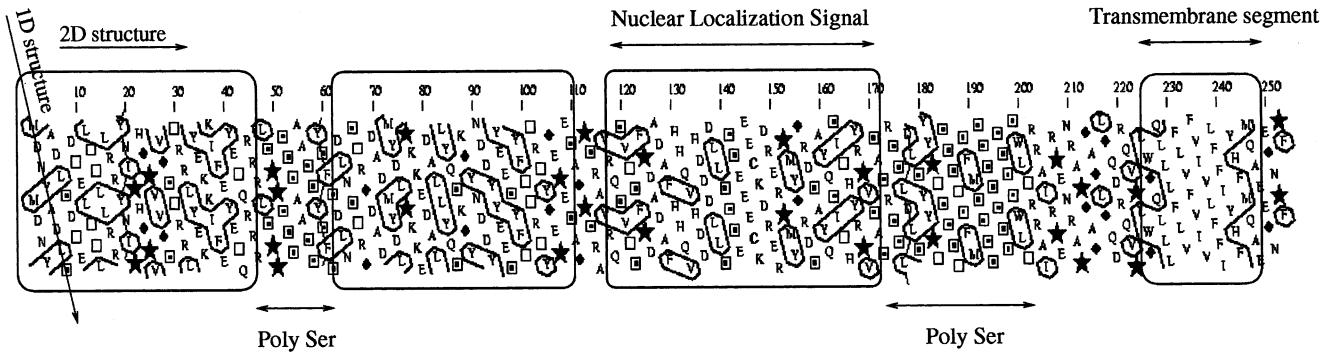

Fig. 1. General organization of emerin as predicted from the analysis of its hydrophobic cluster analysis (HCA) plot [31]. HCA readily detects an N-terminal globular domain (box 1), then a poly-Ser region, a segment of 100 residues rich in hydrophobic amino acids (boxes 2 and 3) comprising the nuclear localization signal ([7,8], box 3), again a poly-Ser region, and finally a transmembrane segment (box 4). The protein sequence is shown on a duplicated α-helical net with amino acid positions indicated above. The contours of the hydrophobic residues are automatically drawn to form clusters that mainly correspond to the internal faces of regular secondary structures [32]. Symbols: open square, threonine; square with dot inside, serine; diamond, glycine; star, proline.

sional structures. This procedure is described in detail in Savarin et al. [29]. A force field adapted to NMR structure calculation (files topallhdg.pro and parallhdg.pro in X-PLOR 3.1) was used. At the last step, 200 structures were calculated and the 10 best structures were selected to be analyzed.

3. Results

3.1. Is the N-terminal domain monomeric in solution?

Analytic ultracentrifugation was used in order to characterize the oligomerization state of the emerin N-terminal domain. At equilibrium, a mass corresponding to a monomer was measured. Thus, the N-terminal domain of emerin does not self-associate at pH 6.3 and for a concentration lower than 50 μM.

3.2. Proton–proton distances deduced from NOESY experiments

On the NOESY spectra, 3017 (2035 in H_2O, 982 in D_2O) peaks were analyzed. At the end of the assignment and structure calculation procedure, 116 peaks remained unassigned. Eighty-five peaks correspond to unknown chemical shifts, probably characteristic of minor conformations, and 19 to distances which are higher than 7 Å on the three-dimensional structures. On the basis of the 2913 other peaks, 1219 restraints were generated. Ten restraints were not used in the calculations because they led to systematic violations higher than 0.5 Å. The structures were calculated on the basis of the 1209 remaining distance restraints, which comprised 87 ambiguous restraints at the last iteration. The mean number of unambiguous distance restraints per residue yielded 22.8.

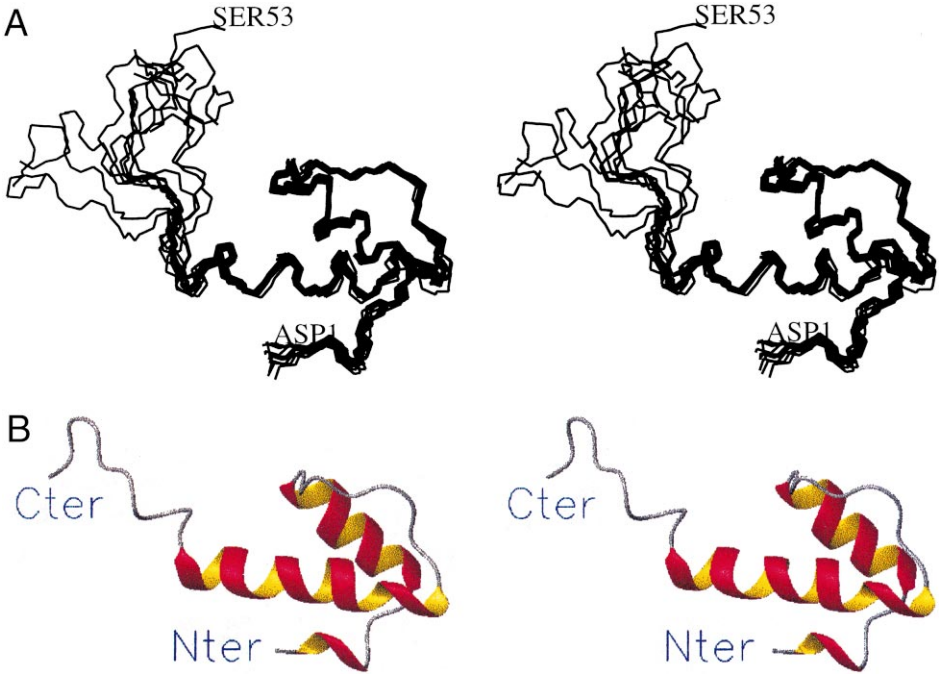

Fig. 2. A: Stereoview of the 10 final backbone structures of the emerin N-terminal domain. B: Ribbon representation (in stereo [33]) of the averaged structure of the emerin N-terminal domain.

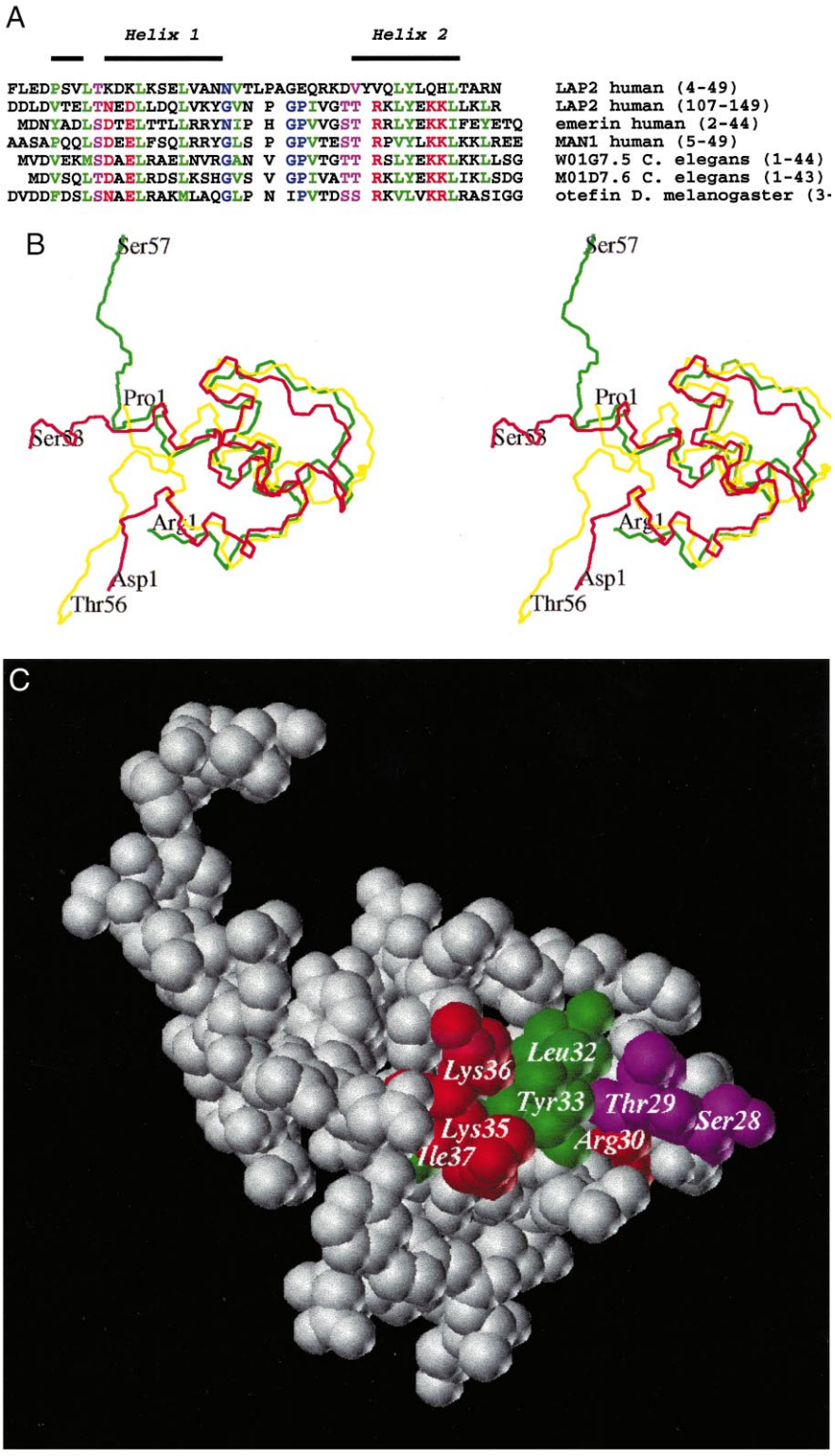

Fig. 3. A: Multiple alignment of LEM-like and LEM domains. Conserved hydrophobic residues are displayed in green, conserved charged residues in red, conserved polar and neutral residues in magenta and conserved glycines and prolines in blue. B: Stereoview of the backbone structures of the LEM-like domain of LAP2 (in yellow), the LEM domain of LAP2 (in red) and the LEM domain of emerin (in green). The three structures were fitted on the backbone atoms of residues 1–21, 23–29, 30–41 in emerin and the corresponding residues in the LEM-like and LEM domains of LAP2. C: A conserved solvent-exposed surface observed on LEM domain structures. Residues of the emerin N-terminal domain conserved in all LEM domains are colored red, magenta and green when they are positively charged, polar/neutral, and hydrophobic, respectively.

3.3. Structural statistics

Analysis of the 10 final structures (Table 1) of the emerin N-terminal domain shows that no distance violations larger than 0.5 Å are present. Furthermore, the covalent geometry is respected, as evidenced by the low RMSD value for bond lengths and valence angles. The value of the van der Waals energy is small, indicating that there is no incorrect non-bonded contacts.

3.4. Backbone structure

A backbone superposition of the 10 lowest-energy structures of the emerin N-terminal domain is shown in Fig. 2A. The conformation of the backbone (C, N, Cα atoms) is well defined for residues 1–43: the RMSD with respect to the mean coordinates is close to 0.6 ± 0.1 Å. The Ramachandran plot of the protein segment 1–43 confirms the good quality of the structures as no residues are systematically in the disallowed region. Over the 10 structures, the percentage of residues in the most favored and additional allowed region is 99.7%.

A three-residue N-terminal 3_{10} helix and two large α-helices, named helix 1 and helix 2, are observed in emerin (Fig. 2B). Inspection of the Ramachandran map shows that the three helical segments comprise residues Asn2–Asp5 (N-terminal helix), Asp8–Tyr18 (helix 1) and Gly27–Gln43 (helix 2). A characteristic $i \rightarrow i+3$ hydrogen bond is observed between residues 2 and 5 in the N-terminal helix. The large helices 1 and 2 are α-helices. They are stabilized by six $i \rightarrow i+4$ hydrogen bonds present in segment 7–16 of helix 1, and 11 $i \rightarrow i+4$ hydrogen bonds present at more than 70% in segment 29–43 of helix 2.

3.5. Side chains

The hydrophobic core of the emerin N-terminal domain is formed by a large number of leucine residues (Leu6, 11, 14, 15), assisted by additional valine (Val25), isoleucine (Ile20 and 37) and tyrosine (Tyr18, 33, 40) residues. Two polar side chains, His22 and Glu34, are also more than 80% buried in the structure. Glu34 makes a salt bridge with Arg30.

4. Discussion

4.1. Emerin N-terminal domain adopts the LEM fold

The emerin N-terminal domain is significantly related to several domains of proteins anchored in the inner nuclear membrane ([23], see Fig. 3A). It is similar to (i) the two N-terminal domains of human LAP2 (identities of sequence: 16 and 34%) and the N-terminal domain of human MAN-1 (identity: 41%), (ii) the N-terminal domains of *Caenorhabditis elegans* M01D7.6 (identity: 39%) and W01G7.5 (identity: 34%), and (iii) the N-terminal domain of *Drosophila melanogaster* otefin (identity: 25%). All these domains are predicted to adopt a common fold, called the LEM fold. Recently, we have experimentally proven that the two N-terminal domains of human LAP2, although highly divergent in sequence, have similar solution structures, and we have shown that their three-dimensional structures mainly consist of two large parallel α-helices [30]. This work establishes that the N-terminal domain of emerin also adopts the LEM fold.

Superimposition of the so-called LEM-like (residues 1–56) and LEM domains (103–151) of LAP2 with the LEM domain of emerin is displayed in Fig. 3B. The positioning of the short N-terminal helix and the two main α-helices is conserved in the three domains. The root mean square deviation calculated on the backbone atoms between the α-helices of emerin and LAP2 LEM domain is equal to 1.1 Å; it is 1.7 Å on the whole backbone. When comparing emerin to the LAP2 LEM-like domain, the same calculations yield 1.9 and 3.0 Å, respectively. Comparison of the LAP2 LEM-like and LEM domains yields similar values of 1.7 and 3.1 Å, respectively. These higher values are due to a slightly different orientation of helix 2, evaluated to be 15°, in the LEM-like domain when compared to the LEM domains of emerin and LAP2.

Comparison of the LEM domain sequences shows that eight positions are systematically hydrophobic (Fig. 3A). The N-terminal three-residue helix is stabilized by the interaction of the first two conserved hydrophobic residues with the hydrophobic core of the domain, and the six remaining conserved hydrophobic residues are buried due to the interaction of helix 1 with helix 2. A continuous segment, formed by residues Thr/Ser36, Arg37, Leu/Val39, Tyr/Leu40, Lys42, Lys/Arg43 and Leu/Ile44, is also highly conserved (Fig. 3A). This positively charged segment corresponds to the solvent-exposed surface of helix 2 (Fig. 3C). It could thus be the interaction site of LEM domains with a common partner. Interestingly, most of the residues within this conserved segment are not found in the LEM-like domain of LAP2 (residues 4–49), suggesting that LEM-like and LEM domains have different biological targets.

4.2. Functional role of emerin LEM domain

Emerin was shown in vitro to bind to lamin A and BAF. In the case of lamin A, it is known that the 188 first amino acids of emerin, comprising the LEM domain, the poly-Ser and the 100-residue domain are sufficient for binding to region 384–566 of lamin A [18,19]. In the case of BAF, mutations in the LEM domain disrupt emerin binding [15]. Similarly, the N-terminal region of LAP2 comprising the LEM-like and LEM domains interacts with BAF alone and with a BAF/DNA complex. Mutations in the LAP2 LEM domain either before the $^{3}10$ helix, at the C-terminus of helix 1, in the loop between helices 1 and 2, or in helix 2 disrupt BAF binding. Thus, a consensus appears for a role of LEM domains in protein–protein interaction. In particular, the LEM domains of LAP2 and emerin interact with protein BAF, and as the homology within LEM domains is high (25–41% identity relative to the emerin LEM domain), this might be a general property of LEM domains. Further experiments are needed to characterize the LEM–BAF interaction at an atomic level.

Acknowledgements: We thank Gérard Battelier for technical assistance, Cecilia Östlund for helpful input and Jean-Claude Courvalin for invaluable discussions. H.J.W. was supported by a grant from the Muscular Dystrophy Association.

References

[1] Emery, A.E.H. (1989) J. Med. Genet. 26, 637–641.
[2] Emery, A.E.H. (1996) in: Principles and Practices of Medical Genetics, 3rd edn. (Rimon, D.L., Connor, J.M. and Pyeritz, R.E., Eds.), pp. 2337–2354. Churchill Livingstone, Edinburgh.
[3] Manilal, S., Nguyen, T.M., Sewry, C.A. and Morris, G.E. (1996) Hum. Mol. Genet. 5, 801–808.
[4] Nagano, A., Koga, R., Ogawa, M., Kurano, Y., Kawada, J., Okada, R., Hayashi, Y.K., Tsukahara, T. and Arahata, K. (1996) Nature Genet. 2, 254–259.

[5] Bione, S., Maestrini, E., Rivella, S., Mancini, M., Regis, S., Romeo, G. and Toniolo, D. (1994) Nature Genet. 8, 323–327.
[6] Bonne, G., Di Barletta, M.R., Varnous, S., Becane, H.M., Hammouda, E.H., Merlini, L., Muntoni, F., Greenberg, C.R., Gary, F., Urtizberea, J.A., Duboc, D., Fardeau, M., Toniolo, D. and Schwartz, K. (1999) Nature Genet. 21, 285–288.
[7] Östlund, C., Ellenberg, J., Hallberg, E., Lippincott-Schwartz, J. and Worman, H.J. (1999) J. Cell Sci. 112, 1709–1719.
[8] Tsuchiya, Y., Hase, A., Ogawa, M., Yorifuji, H. and Arahata, A. (1999) Eur. J. Biochem. 259, 859–865.
[9] Gerace, L. and Foisner, R. (1994) Trends Cell Biol. 6, 347–353.
[10] Worman, H.J., Yuan, J., Blobel, G. and Georgatos, S.D. (1988) Proc. Natl. Acad. Sci. USA 85, 8531–8534.
[11] Worman, H.J., Evans, C.D. and Blobel, G. (1990) J. Cell Biol. 111, 1535–1542.
[12] Foisner, R. and Gerace, L. (1993) Cell 73, 1267–1279.
[13] Furukawa, K. (1999) J. Cell Sci. 112, 2485–2492.
[14] Dechat, T., Vlcek, S. and Foisner, R. (2000) J. Struct. Biol. 129, 335–345.
[15] Shumaker, D.K., Lee, K.K., Tanhehco, Y.C., Craigie, R. and Wilson, K.L. (2001) EMBO J. 7, 1754–1764.
[16] Fairley, E.A., Kendrick-Jones, J. and Ellis, J.A. (1999) J. Cell Sci. 112, 2571–2582.
[17] Sullivan, T., Escalante-Alcalde, D., Bhatt, H., Anver, M., Bhat, N., Nagashima, K., Stewart, C.L. and Burke, B. (1999) J. Cell Biol. 147, 913–920.
[18] Clements, L., Manilal, S., Love, D.R. and Morris, G.E. (2000) Biochem. Biophys. Res. Commun. 267, 709–714.
[19] Sakaki, M., Koike, H., Takahashi, N., Sasagawa, N., Tomioka, S., Arahata, K. and Ishiura, S. (2001) J. Biochem. (Tokyo) 129, 321–327.
[20] Boyle, S., Gilchrist, S., Bridger, J.M., Mahy, N.L., Ellis, J.A. and Bickmore, W.A. (2001) Hum. Mol. Genet. 10, 211–219.
[21] Ellis, J.A., Craxton, M., Yates, J.R. and Kendrick-Jones, J. (1998) J. Cell Sci. 111, 781–792.
[22] Manilal, S., Nguyen, T.M. and Morris, G.E. (1998) Biochem. Biophys. Res. Commun. 249, 643–647.
[23] Lin, F., Blake, D.L., Callebaut, I., Skerjanc, I.S., Holmer, L., McBurney, M.W., Paulin-Levasseur, M. and Worman, H.J. (2000) J. Biol. Chem. 275, 4840–4847.
[24] Rance, M., Sorensen, O.W., Bodenhausen, G., Wagner, G., Ernst, R.R. and Wüthrich, K. (1983) Biochem. Biophys. Res. Commun. 117, 479–485.
[25] Braunschweiler, L. and Ernst, R.R. (1983) J. Magn. Reson. 53, 521–528.
[26] Kumar, A., Ernst, R.R. and Wüthrich, K. (1980) Biochem. Biophys. Res. Commun. 95, 1–6.
[27] Piotto, M.., Saudek, V. and Sklenar, V. (1992) J. Biomol. NMR 2, 661–665.
[28] Gilquin, B., Lecoq, A., Desné, F., Guenneugues, M., Zinn-Justin, S. and Ménez, A. (1999) Proteins 34, 520–532.
[29] Savarin, P., Zinn-Justin, S. and Gilquin, B. (2001) J. Biomol. NMR 19, 49–62.
[30] Laguri, C., Gilquin, B., Wolff, N., Romi-Lebrun, R., Courchay, K., Callebaut, I., Worman, H.J. and Zinn-Justin, S. (2001) Structure 9, 503–511.
[31] Gaboriaud, C., Bissery, V., Benchetrit, T. and Mornon, J.P. (1987) FEBS Lett. 224, 149–155.
[32] Callebaut, I., Labesse, G., Durand, P., Poupon, A., Canard, L., Chomilier, J., Henrissat, B. and Mornon, J.P. (1997) Cell. Mol. Life Sci. 53, 621–645.
[33] Koradi, R., Billeter, M. and Wüthrich, K. (1996) J. Mol. Graph. 14, 51–55.
[34] Laskowski, R.A., Rullmannn, J.A., MacArthur, M.W., Kaptein, R. and Thornton, J.M. (1996) J. Biomol. NMR 8, 477–486.